

1 **Mixed communities of mucoid and non-mucoid *Pseudomonas aeruginosa* exhibit enhanced**  
2 **resistance to host antimicrobials.**

3 Sankalp Malhotra, Dominique H. Limoli, Anthony English, Erin Mulroney, Daniel J. Wozniak.

4  
5 **Abstract**

6 *Pseudomonas aeruginosa* (*P.a.*) is a bacterial pathogen that causes chronic lung infections in  
7 cystic fibrosis (CF) patients. The CF lung is hyperinflammatory due to an abundance of  
8 neutrophil-derived antimicrobials, including reactive oxygen species [e.g. hydrogen peroxide  
9 (H<sub>2</sub>O<sub>2</sub>)] and antimicrobial peptides (e.g. LL-37). *P.a.* colonizes the CF lung by acquiring  
10 adaptive mutations. Mutation of *mucA* results in a mucoid phenotype due to the overproduction  
11 of the polysaccharide alginate. Mucoid isolates often revert to a nonmucoid phenotype through  
12 second mutations. Mucoid and nonmucoid strains are often isolated from the same patient  
13 sample, suggesting a selective advantage for the co-existence of these variants in the CF lung.  
14 We hypothesized that mucoid/non-mucoid *P.a.* may be differentially susceptible to neutrophil  
15 products, exhibiting heightened resistance to host factors in consortia. While clinical mucoid *P.a.*  
16 isolate (FRD1) was 10-fold more resistant to LL-37 compared to non-mucoid variants, FRD1  
17 was also more sensitive to H<sub>2</sub>O<sub>2</sub> compared to a non-mucoid, *algT* revertant. Resistance to H<sub>2</sub>O<sub>2</sub>  
18 was dependent on catalase (*katA*) expression, which was likely regulated by two transcription  
19 factors, AlgT and AlgR. Extracellular release of KatA was found to be dependent on the  
20 expression of *lys*, which encodes an endolysin in *P.a.* already implicated in eDNA release. Co-  
21 cultures of mucoid/non-mucoid strains (mimicking CF lung co-isolates) exhibited greater  
22 tolerance to both H<sub>2</sub>O<sub>2</sub> and LL-37 than mono-culture. These data provide an important rationale  
23 to study the interaction of mucoid/non-mucoid *P.a.* variants as contributors to CF pathology.

## 24 **Introduction**

25 Cystic fibrosis (CF) is a lethal genetic disease that manifests in early childhood and  
26 progresses to multi-organ dysfunction, lung failure, and premature death<sup>1</sup>. There are currently  
27 30,000 patients living with CF in the United States (70,000 globally), with nearly 1000 new  
28 diagnoses each year<sup>2</sup>. Despite progress in diagnosis and management strategies, morbidity and  
29 mortality in CF continue to be closely associated with chronic respiratory infections complicated  
30 by antimicrobial resistance<sup>3</sup>. From infancy, CF patients suffer from accumulation of thick, dried  
31 mucus within their airways, which leads to entrapment of opportunistic bacteria<sup>4</sup>. During the  
32 chronic stages of disease, the Gram-negative bacterium *Pseudomonas aeruginosa* (*P.a.*)  
33 predominates in the CF lung, exacerbating pathology and hastening patient mortality<sup>5</sup>. The  
34 progression of CF lung disease is driven by a combination of host and bacterial factors. Infection  
35 with *P.a.* promotes excessive influx of neutrophils into the lung, which drives tissue damage,  
36 fibrosis, and compromised function<sup>6</sup>. Importantly, neutrophils in CF overproduce antimicrobials  
37 like reactive oxygen species (ROS) [e.g. hydrogen peroxide (H<sub>2</sub>O<sub>2</sub>) and hypochlorite (HOCl)]  
38 that are damaging to both the host and bacteria<sup>7</sup>. Neutrophils also produce LL-37, an  
39 antimicrobial peptide that functions both as an innate immune effector as well as an  
40 immunomodulator<sup>6</sup>.

41 *P.a.* successfully colonizes the hyper-inflammatory environment of the CF lung via  
42 acquisition of stable mutations<sup>8</sup>. One striking *P.a.* adaptation occurs via mutation of the gene  
43 *mucA*, resulting in over-production of the bacterial exopolysaccharide, alginate<sup>9</sup>. This phenotypic  
44 switch from an alginate non-producing (non-mucoid) to an alginate-overproducing (mucoid)  
45 phenotype has negative consequences for CF patients<sup>10</sup>. Compared to non-mucoid isolates,  
46 mucoid *P.a.* exhibits enhanced resistance to multiple antibiotics<sup>11</sup> and to innate immune

47 effectors<sup>10</sup>, including antimicrobial peptides. As such, mucoid conversion is also correlated with  
48 a dramatic decline in patient lung function and marks a transition to the chronic and  
49 progressively debilitating stages of disease<sup>12</sup>. In addition to the alginate polysaccharide, *P.a.*  
50 expresses enzymes that also protect it from the host response, including catalases encoded by  
51 *katA* and *katB*<sup>13</sup> that combat H<sub>2</sub>O<sub>2</sub>-stress.

52         Despite the well-documented recalcitrance of the mucoid *P.a.* phenotype, both mucoid  
53 and non-mucoid *P.a.* are often isolated together in CF patient sputum<sup>14</sup>. Non-mucoid *P.a.* present  
54 in the CF lung in chronic disease are often non-mucoid “revertants” that have acquired a second  
55 site mutation (following mucoid conversion via *mucA*). These second-site mutations often occur  
56 both *in vitro* and *in vivo* in the gene, *algT*, which encodes the central sigma factor responsible for  
57 mucoid conversion<sup>15</sup>. Functional AlgT is required to up-regulate the alginate biosynthetic  
58 operon, which begins with the gene *algD*. *mucA* encodes an anti-sigma factor that normally  
59 sequesters AlgT at the inner membrane. Mutation of *mucA* liberates AlgT, which can then up-  
60 regulate alginate biosynthesis<sup>10,16</sup>.

61         AlgT is known to regulate multiple genes outside of the alginate biosynthetic operon as  
62 well. The AlgT regulon is predicted to consist of 300 ORFs<sup>17</sup>. However, downstream of AlgT,  
63 there are three known transcriptional regulators, encoded by the genes *algB*, *algR*, and *amrZ*, that  
64 also positively regulate alginate biosynthesis<sup>18</sup>.

65         Given that mucoid/non-mucoid revertants of *P.a.* are co-isolated from CF lungs, we  
66 hypothesized that there may be an advantage for these multi-variant communities in evasion of  
67 the host response. Here, we show that mucoid *P.a.* resistance to LL-37 is alginate-dependent,  
68 whereas susceptibility to H<sub>2</sub>O<sub>2</sub> is *algT*-dependent. *algT* mutants (non-mucoid revertants)  
69 produce KatA, which is released into the extracellular space in a cell-lysis dependent process that

70 relies on a bacteriophage endolysin encoded within the *P.a.* chromosome. We provide evidence  
71 that *katA* is transcriptionally regulated by *algR*. Finally, we show that mucoid/non-mucoid *P.a.*  
72 variants in consortia are more resistant to LL-37 and H<sub>2</sub>O<sub>2</sub> than in single-variant, mono-cultures.  
73 These findings provide important insights regarding multi-variant *P.a.* interactions that enable  
74 this bacteria to evade critical components of the host-immune response.

75

## 76 **Materials and methods**

77

78 **Strains and growth conditions.** All *P. a.* strains used were streaked for isolation from frozen  
79 stocks at -80 degrees C onto *Pseudomonas* Isolation Agar (PIA), followed by growth in Luria  
80 Broth No Salt (LBNS) medium. *E. coli* (Hb101) strains were streaked for isolation from frozen  
81 stocks onto Luria Agar (LA), followed by growth in Luria Broth (LB). All gene mutations were  
82 made as previously described by overlap extension PCR<sup>19</sup>. When necessary to maintain a  
83 plasmid, *E. coli* strains were grown in LB with 100ug/mL ampicillin. *P.a.* strains with plasmid  
84 were grown in LBNS with 300ug/mL carbenicillin.

85

86 **Alginate purification and quantitation.** *P.a.* alginate was purified as previously described<sup>20</sup>.  
87 Briefly, clinical mucoid isolate, FRD1, was streaked on PIA and grown at 37 degrees C for 16-  
88 18 hours. Colonies were scraped directly from the solid medium and homogenized in 2mL  
89 0.85% saline. Each 1mL of saline and bacteria collected from the plate was split into two equal,  
90 500uL fractions and vortexed well. Bacterial cells were pelleted by centrifugation at 14,000 rpm  
91 for 30 minutes at room temperature. 500 uL 2% cetyl pyridinium chloride was added to the  
92 supernatant to precipitate the alginate (appeared as stringy, white substance). Tubes were

93 inverted to mix, then centrifuged at 14,000 rpm for 10 minutes at room temperature. The  
94 supernatant was discarded and the pellet (alginate) was dissolved in 500 uL of cold (-20 degrees  
95 C) 100% isopropanol. Here, the alginate partially dissolved, and appeared cloudy, white. The  
96 mixture was centrifuge at 14,000 rpm for 10 minutes at room temperature, followed by  
97 discarding the supernatant and draining the tube well. The alginate pellet was resuspended in 500  
98 uL of saline and incubated 12-24 hours at 4 degrees C to become hydrated.

99 *P.a.* alginate was quantitated as described previously<sup>20</sup>. Brown algae-derived (seaweed)  
100 alginate was dissolved in saline and diluted two fold (2mg/mL to 62.5mg/mL) to generate  
101 standards. 50uL of alginate standards or sample were placed in duplicate into a 96-well plate.  
102 200 uL of 25 mM sodium tetraborate in sulfuric acid to each well, followed by mixing the plate  
103 on a nutator. The plate was heated on a standard heatblock at 100 degrees C for 15 minutes, and  
104 allowed to cool to room temperature for 15 minutes. 50uL 0.1% carbazole was then added into  
105 each well, followed by heating the plate at 100 degrees C for 15 minutes. After cooling the plate  
106 to room temperature, absorbance was read on a Spectramax plate reader at wavelength of 550nm.

107

108 **One hour bacterial killing.** Bacterial strains were sub-cultured from overnight growth in LB or  
109 LBNS into fresh medium and grown to exponential phase (approximately  $OD_{600} \approx 0.5$  or  
110  $2 \times 10^8$  CFUs/mL). For H<sub>2</sub>O<sub>2</sub> killing assays, bacteria were then mixed 1:1 with H<sub>2</sub>O<sub>2</sub> diluted in  
111 LBNS (or LBNS alone, i.e. no treatment) and incubated for 1 hour at 37 degrees C, followed by  
112 plating on PIA to quantitate CFUs/mL. Data were expressed as log-fold killing relative to the no-  
113 treatment condition. For the LL-37 killing assays, bacteria at exponential phase were pelleted at  
114 14,000 RPM for 3 minutes and resuspended in sodium phosphate buffer (SPB) at pH 6.4.  
115 Bacteria were then mixed 1:1 with LL-37 diluted in SPB (or in SPB alone) and incubated 1 hour

116 at 37 degrees C, followed by plating on solid medium (PIA for *P.a.* and LA for *E. coli*) to  
117 quantitate CFUs/mL.

118

119 **Mono- vs. co-culture bacterial killing.** Mono- vs co-culture killing assays were performed  
120 identically to the one hour killing assay protocol as described above. In the co-culture  
121 conditions, mucoid/non-mucoid *P.a.* strains were mixed 1:1 prior to exposure to either LL-37 or  
122 H<sub>2</sub>O<sub>2</sub>. Additionally, the mucoid/non-mucoid strains used here were differentially drug-marked  
123 to track their survival in the co-culture condition. The mucoid, FRD1, strain used was a  
124 spontaneous streptomycin resistant isolate, plated on PIA containing 150ug/mL streptomycin to  
125 quantitate CFUs/mL. The isogenic non-mucoid strains (*algT* and *algD* mutants) used were  
126 spontaneous rifampicin resistant isolates, plated on PIA containing 100ug/mL rifampicin to  
127 quantitate CFUs/mL.

128

129 **Biolog growth inhibition and supernatant protection assays.** Bacterial strains grown  
130 overnight (14-16 hours) in LBNS were diluted in fresh medium to OD<sub>600</sub> of 0.24. To generate a  
131 master mix for each bacterial strain, per manufacturer's recommendations: 150uL of bacterial  
132 culture at OD 0.24 was added to 850uL LBNS with 12uL of 10X Biolog Dye (A). 50uL/well of  
133 these bacterial master mixes were added in triplicate to the Biolog 96-well plate. 50uL/well of  
134 H<sub>2</sub>O<sub>2</sub> (diluted in LBNS at desired concentration) or LBNS alone was then added to each well  
135 containing bacteria. Plates were placed in the OmniLog incubator at 37 degrees C for 24 hours.  
136 The Biolog Dye is tetrazolium-based, and detects extracellular metabolites produced during of  
137 growth, resulting in a colorimetrically detectable byproduct. The output of the system is bacterial  
138 growth curves, which can be plotted (as Biolog units versus time in hours) using Biolog's kinetic

139 software (OL\_FM\_12) package. Each growth curve can be converted to parameters including  
140 area under the curve (AUC), maximum growth, maximum slope, and lag time via Biolog's  
141 parametric (OL\_PR\_12) software. AUC was used here as the most representative parameter  
142 corresponding to bacterial growth. Percent survival was calculated by taking the AUC of  
143 bacterial growth in the presence of H<sub>2</sub>O<sub>2</sub> as a percentage of the no-treatment condition for each  
144 strain tested.

145 To assess if bacterial supernatants from various strains are sufficient to protect FRD1  
146 from H<sub>2</sub>O<sub>2</sub>-stress, bacterial strains grown overnight (14-16 hours) in LBNS were centrifuged at  
147 14,000 RPM for 3 minutes to pellet bacterial cells. Supernatants were collected and filter-  
148 sterilized via 0.2µm pore-size filters. FRD1 grown overnight (14-16 hours) in LBNS was diluted  
149 in fresh medium to OD<sub>600</sub> of 0.24. 500µL of this FRD1 culture was pelleted and resuspended  
150 with 500µL of supernatant from desired strains. A master mix with Biolog Dye A was then made  
151 as specified above: 150µL of FRD1 (resuspended in supernatant) was added to 850µL LBNS  
152 with 12µL of 10X Biolog Dye A. 50µL/well of these bacterial master mixes were added in  
153 triplicate to the Biolog 96-well plate, with 50µL/well of H<sub>2</sub>O<sub>2</sub> (diluted in LBNS at desired  
154 concentration) or LBNS alone. Plates were placed in the OmniLog incubator at 37 degrees C for  
155 24 hours. Data were plotted as bacterial growth curves or as percent survival (AUC) as described  
156 above. For each type of Biolog assay, three independent experiments were performed in  
157 triplicate.

158

159 **Reverse transcriptase-PCR.** RT-PCR was performed to measure mRNA levels of desired genes  
160 in bacterial strains of interest as described previously<sup>18</sup>. Here, bacterial strains were grown to  
161 exponential phase (OD<sub>600</sub>= ~0.5-0.8). Bacterial cells were pelleted by centrifugation, and

162 resuspended/lysed in TRIzol for 5 minutes. Chloroform was added and the aqueous phase  
163 containing RNA was collected and applied to the genomic DNA eliminator column provided in  
164 the Qiagen RNeasy Kit. The column was centrifuged at 8000 x g for 30 seconds at 4 degrees C.  
165 The column was then discarded and 1 volume of 70% ethanol was added to the eluent. This  
166 sample was then applied to the RNeasy mini column (pink column). Following centrifugation,  
167 the column was washed with Buffer RW1 twice and then with Buffer RPE twice (with spins as  
168 above between each wash). An empty column spin for 2 minutes was performed to dry the  
169 RNeasy silica-gel membrane. The column was then transferred to a new collection tube and  
170 RNA was eluted with 50uL RNase-free water.

171         The RNA preparations were then converted to cDNA using the Thermo SuperScript III  
172 First-Strand Synthesis System, per manufacturer's instructions. Real time PCR was performed  
173 using Bio-Rad CFX1000 thermal cycler, gene-specific primer pairs, and SYBR green supermix.  
174 All samples were normalized to housekeeping gene *rpoD* and mRNA transcript fold-change was  
175 calculated relative to FRD1. All experiments were performed in triplicate on three independent  
176 occasions.

177

178 **Catalase activity assays.** To measure catalase protein activity in the cell-free supernatants of  
179 *P.a.* strains, a commercially available kit (BioVision Catalase Activity  
180 Colorimetric/Fluorometric Assay) was used per manufacturer's instructions. Supernatants were  
181 diluted 1:4 in assay buffer and added to a 96 well plate to a final volume of 78uL. A H<sub>2</sub>O<sub>2</sub>  
182 standard curve was generated to include 0, 2, 4, 6, 8, and 10 nmol/well, also to a final volume of  
183 78uL/well. 10uL of stop solution was added into the wells containing the standards. The positive  
184 control was catalase enzyme (diluted 1:16 in assay buffer). One additional well included the



185 catalase enzyme with stop solution (this was treated as the “high control” or negative control).  
186 12uL fresh 1mM H<sub>2</sub>O<sub>2</sub> was added into each well (samples and positive control) to start the  
187 reaction and incubated at room temperature for 30 minutes. 10uL of stop solution was then added  
188 into each sample well. Finally, for each well, a 50uL developed mix containing 46uL assay  
189 buffer, 2uL OxiRed Probe, and 2uL HRP solution was prepared and added to samples, controls,  
190 and standards. After 10 minutes of incubation at room temperature, absorbance was measured at  
191 OD 570nm using a Spectramax plate reader. Catalase activity was calculated by first calculating  
192 signal change:  $\Delta A = \text{absorbance of the high control} - \text{absorbance of each sample}$ . After plotting  
193 the standard curve, linear regression was used to convert  $\Delta A$  to get B nmol of H<sub>2</sub>O<sub>2</sub> decomposed  
194 by catalase in a 30 minute reaction. Catalase activity could then be calculated as follows:  
195 Catalase activity =  $B/30 \times V \times \text{Sample dilution factor} = \text{nmol/min/mL} = \text{mU/mL}$ , where one unit of  
196 catalase decomposes 1umol of H<sub>2</sub>O<sub>2</sub> per minute at pH 4.5 at 25 degrees C.

197

## 198 **Results**

199

200 **Alginate is sufficient to protect bacteria from LL-37 killing.** We had previously shown that  
201 mucoid isolates of *P.a.* were more resistant to LL-37 mediated killing (at lethal doses) compared  
202 to isogenic, non-mucoid variants<sup>21</sup>. Here, we sought to determine if the exopolysaccharide,  
203 alginate, which is produced in excess by mucoid *P.a.*, is sufficient to protect non-mucoid *P.a.*  
204 from LL-37 stress. We purified alginate from a clinical, mucoid isolate, FRD1, and added it  
205 exogenously to an isogenic, *algD* mutant (at multiple concentrations) prior to exposing these  
206 strains to LL-37 for 1 hour. Bacteria were then plated for CFUs/mL on PIA and log-fold killing  
207 was calculated relative to no-treatment for each condition. As shown in our previous publication,

208 the *algD* mutant alone was 1-log more sensitive to LL-37 compared to the mucoid isolate.  
209 However, *P.a.*-derived alginate was sufficient to protect the *algD* mutant, even at the lowest  
210 added concentration of 10ug/mL (Fig. 1A). Here, we used three concentrations of alginate:  
211 250ug/mL, 100ug/mL, and 10ug/mL. Alginate quantitation in CF patient sputum has shown a  
212 range of 10ug/mL to 100ug/mL of alginate<sup>22</sup>, and an FRD1 culture grown to stationary phase  
213 contains approximately 250ug/mL alginate, which is a concentration used in prior work as  
214 well<sup>23</sup>. Notably, commercially available alginate derived from brown algae, which differs from  
215 *P.a.* alginate only in its acetylation state (i.e. it is still a polymer of mannuronic and guluronic  
216 acid), was sufficient to protect *E. coli* from LL-37 killing (Fig. 1B). This suggests that bacterial  
217 resistance to LL-37 is alginate-dependent and that this phenomenon is independent of bacterial  
218 genera.

219  
220 ***algT* mutation confers resistance to H<sub>2</sub>O<sub>2</sub>.** Given that the alginate polysaccharide provided  
221 protection from LL-37, we proposed that it may be similarly protective against other neutrophil-  
222 produced antimicrobials such as ROS. Here, we used a high-throughput system called Biolog to  
223 investigate the capacity of isogenic mucoid *P.a.* isolate FRD1, and two non-mucoid strains (*algT*  
224 and *algD* mutants) to grow for 24 hours in the presence of two distinct ROS: HOCl and H<sub>2</sub>O<sub>2</sub>.  
225 The resulting bacterial growth curves (Supplemental Figure 1) were converted into to the  
226 parameter of area under the curve (AUC), which taken as a percentage of the no-treatment  
227 conditions provided an output of percent survival. We found that growth of all three strains was  
228 similar in the presence of 11.25mM of HOCl. Surprisingly, however, the *algT* strain was  
229 significantly more resistant to growth in the presence of 25mM H<sub>2</sub>O<sub>2</sub> compared to both the  
230 mucoid and *algD* strains. To validate Biolog as an effective means to investigate bacterial

231 susceptibility to ROS, we exposed all three strains to a lethal dose of H<sub>2</sub>O<sub>2</sub> (50mM) for 1 hour,  
232 plated surviving bacteria for CFUs/mL, and computed log-fold killing relative to no-treatment  
233 for each condition. Here too, we found that the *algT* strain was least susceptible to H<sub>2</sub>O<sub>2</sub>-killing  
234 compared to the mucoid and *algD* mutants. These findings suggest that H<sub>2</sub>O<sub>2</sub> susceptibility in  
235 *P.a.* is *algT*-dependent and independent of mucoid status.

236

### 237 **Various clinical mucoid *P.a.* isolates demonstrate susceptibility to H<sub>2</sub>O<sub>2</sub>, similar to FRD1.**

238 Given that mucoidy appeared to be non-protective versus H<sub>2</sub>O<sub>2</sub> killing, we wanted to investigate  
239 whether this phenotype was specific to the clinical mucoid isolate, FRD1, or generalizable across  
240 mucoid *P.a.* strains. Here, we tested the H<sub>2</sub>O<sub>2</sub> susceptibility of a panel of 10 clinical mucoid  
241 isolates (including FRD1) by Biolog. We found that 5/10 strains tested were statistically non-  
242 significant in their H<sub>2</sub>O<sub>2</sub>-susceptibility compared to FRD1, suggesting that a clear subset of  
243 mucoid *P.a.* isolates may be susceptible to H<sub>2</sub>O<sub>2</sub> (Fig. 3). Within this H<sub>2</sub>O<sub>2</sub>-sensitive subset,  
244 each strain was significantly more sensitive to H<sub>2</sub>O<sub>2</sub> compared to the *algT* mutant of FRD1.

245

### 246 **Cell-free supernatants derived from the *algT* mutant protect FRD1 from H<sub>2</sub>O<sub>2</sub> stress via**

247 **KatA.** We hypothesized that the *algT* mutant may be resistant to H<sub>2</sub>O<sub>2</sub> due to the secretion of a  
248 soluble antioxidant. To test this experimentally, we filter-sterilized supernatants from stationary  
249 phase cultures of FRD1, *algT*, and *algD* strains. These supernatants were used to resuspend  
250 FRD1 prior to its growth in the presence of H<sub>2</sub>O<sub>2</sub> for 24 hours. Only supernatants from the *algT*  
251 strains protected FRD1 from H<sub>2</sub>O<sub>2</sub>-killing (Fig. 4A). Furthermore, heat-inactivation of the *algT*  
252 supernatants (by heating at 80 degrees C for 30 minutes) abrogated protection of FRD1 from  
253 H<sub>2</sub>O<sub>2</sub>, suggesting that the soluble factor is a heat-labile protein (Fig 4A). The catalases, KatA

254 and KatB, have been shown to be two vital antioxidants produced by *P.a.* for defense against  
255 H<sub>2</sub>O<sub>2</sub><sup>24</sup>. KatA is a constitutively expressed catalase that is found in both the *P.a.* cytoplasmic  
256 and periplasmic compartments, whereas KatB is an induced catalase that is found only in the *P.a.*  
257 cytoplasm<sup>13</sup>. *katB* expression is regulated by *oxyR* and is dependent on H<sub>2</sub>O<sub>2</sub>-exposure<sup>25</sup>. To  
258 determine whether either KatA or KatB may be the protective factor against H<sub>2</sub>O<sub>2</sub> within *algT*  
259 supernatants, we generated *algT*  $\Delta$ *katA* and *algT*  $\Delta$ *katB* mutants. Supernatants derived from an  
260 *algT*  $\Delta$ *katA* mutant showed abrogated capacity to protect FRD1 against H<sub>2</sub>O<sub>2</sub>, whereas deletion  
261 of *katB* had no effect (Fig 4B). This phenotype was complemented by expression of *katA* in-trans  
262 via a pHERD20T vector (under the control of an arabinose-inducible promoter) (Fig. 4C). This  
263 suggested that supernatants derived from the *algT* mutant protect mucoid *P.a.* via the presence of  
264 KatA.

265

266 ***algT* indirectly represses *katA* transcription via *algR*.** Given that mutation of *algT* resulted in  
267 greater protection of *P.a.* from H<sub>2</sub>O<sub>2</sub> via KatA, we proposed that *algT* may act as a repressor of  
268 *katA* transcription. Though sigma factors do not commonly function to suppress gene  
269 transcription directly, they can negatively regulate gene expression via secondary or downstream  
270 transcription factors. In alginate biosynthesis, three main transcription factors lie downstream of  
271 AlgT: AlgB, AlgR, and AmrZ (Fig 5A). If these transcription factors directly repress *katA*  
272 transcription, we reasoned that mutation of the genes that encode for these factors should result  
273 in increased resistance to H<sub>2</sub>O<sub>2</sub> (i.e. the same effect as an *algT* mutation). We observed that *algR*  
274 mutation specifically results in enhanced resistance to H<sub>2</sub>O<sub>2</sub> (Fig 5B). Additionally, by RT-PCR,  
275 we found that *katA* transcript is up-regulated in both the *algT* and *algR* mutant backgrounds  
276 relative to the isogenic mucoid, FRD1 isolate (Fig 5C). Finally, catalase protein activity was also

277 higher in the cell-free supernatants of the *algT* and *algR* mutants relative to *mucA* (Fig 5D),  
278 suggesting that *algT* is an indirect repressor of *katA* transcription via *algR*.

279

280 **Extracellular release of KatA is dependent on *lys*-mediated explosive cell lysis.** Previous  
281 work had shown that KatA appears to be released from *P.a.* during stationary phase of growth  
282 via cell lysis<sup>25</sup>. However, a clear mechanism for *P.a.* cell lysis as a driver of KatA secretion was  
283 not elucidated. Recently, a bacteriophage endolysin encoded by *lys* (PA0629) has been shown to  
284 mediate explosive cell lysis and eDNA release in *P.a.* (Figure 6A) Here, we sought to investigate  
285 whether *lys* has a role in KatA release in *algT* mutants as well. To this end, we generated both  
286 *algT Δlys* and *Δlys/plys* strains. We first wanted to validate the *Δlys* mutant by confirming that it  
287 has a deficiency in eDNA release. As such, we purified cell-free supernatants from FRD1, *algT*,  
288 *algT Δlys* and *Δlys/plys* strains. These supernatants were combined with 6X DNA running buffer  
289 and subjected to agarose gel electrophoresis. A high molecular weight band was observed for  
290 each of the strains (Fig 6B), which was suggestive of extracellular chromosomal DNA (eDNA).  
291 The intensity of this band (densitometry) was quantitated by ImageJ software (Fig 6C). We  
292 observed that the *algT* mutant appears to undergo more cell lysis (i.e. greater eDNA release) than  
293 the mucoid strain. Furthermore, deletion of *lys* in the *algT* background reduces cell lysis and this  
294 can be complemented by expression of *lys* in-trans under the control of an arabinose-inducible  
295 promoter.

296 We also saw that deletion of *lys* resulted in increased susceptibility to H<sub>2</sub>O<sub>2</sub> (Fig 6D),  
297 and this was likely because of reduced catalase protein activity in the cell-free supernatants of  
298 this mutant (Fig 6E). To our knowledge, this finding for the first time links a specific mechanism  
299 for cell lysis and extracellular release of *P.a.* catalase (KatA). Finally, we wanted to know

300 whether *lys* gene transcription is negatively regulated by *algT/algR* in the same way as *katA*. RT-  
301 PCR showed that *lys* transcript was unchanged in the *algT* and *algR* mutant backgrounds,  
302 relative to the mucoid strain. This observation suggests two non-mutually exclusive  
303 explanations: 1) *lys* may be post-transcriptionally regulated or 2) another gene in the *lys*-  
304 mediated cell lysis pathway (e.g. *hol*, PA0614) may be transcriptionally up-regulated in the  
305 *algT/algR* mutant backgrounds. It has been previously seen that *hol* over-expression is sufficient  
306 to induce cell lysis<sup>26</sup>.

307

308 **Co-cultures of mucoid/non-mucoid isolates, which mimic multi-variant *P.a.* populations**  
309 **within the CF lung, exhibit enhanced resistance to host antimicrobials.** Mucoid and non-  
310 mucoid *P.a.* morphotypes are commonly co-isolated from CF patients, despite the heightened  
311 resistance of mucoid *P.a.* to multiple antimicrobials. As such, we hypothesized that there may be  
312 a selective advantage to co-localization of mucoid/non-mucoid *P.a.* within patient lungs to evade  
313 the host response. To test this, we exposed mono- or co-cultures of mucoid and non-mucoid  
314 variants to either H<sub>2</sub>O<sub>2</sub> or LL-37 for 1 hour, followed by plating for CFUs/mL. In these  
315 experiments, the mucoid (streptomycin-resistant) and non-mucoid (rifampicin-resistant) strains  
316 were differentially drug-marked to easily and independently track their survival in co-culture.

317 In mono-culture, the *algT* strain is clearly more resistant to H<sub>2</sub>O<sub>2</sub> than the mucoid  
318 strains; however, in co-culture, the susceptibility of the mucoid strain to H<sub>2</sub>O<sub>2</sub> is almost identical  
319 to that of the *algT* strain. This is because the *algT* strain is producing KatA, which is likely to be  
320 acting as a common good to protect both the mucoid/non-mucoid *P.a.* within the mixed  
321 community.

322 Similarly, in mono-culture, the mucoid strain is significantly more resistant to LL-37 than  
323 the non-mucoid, *algD* strain. However, in co-culture, the susceptibility of the mucoid and non-  
324 mucoid strain to LL-37 is similar, wherein the *algD* strain is likely rescued by the presence of the  
325 exopolysaccharide, alginate, from the mucoid isolate. As such, based on these *in vitro*  
326 experiments, there appears to be an advantage for multi-variant, mucoid/non-mucoid  
327 communities of *P.a.* for the evasion of two critical innate immune effectors.

328

### 329 **Figure legends**

330

#### 331 **Figure 1. Alginate is sufficient to protect both *P.a.* and *E. coli* from LL-37-mediated killing.**

332 (A) One hour treatment with lethal dose of LL-37 (25ug/mL) of clinical mucoid isolate, FRD1  
333 (*mucA*), isogenic *algD* strain, or *algD* strain plus exogenously added alginate at three different  
334 concentrations (250ug/mL, 100ug/mL, and 10ug/mL), followed by enumeration of surviving  
335 bacteria by plating on Pseudomonas Isolation Agar (PIA) for CFUs. Data are represented as log-  
336 fold killing compared to no-treatment for each strain/condition. To isolate alginate, FRD1  
337 colonies growing on PIA were scraped, homogenized, and alginate precipitated via cetyl  
338 pyridinium chloride. Alginate was quantitated by the carbazole assay. (B) Log-fold killing of *E.*  
339 *coli* strain, Hb101, by three different concentrations of LL-37 with or without the presence of  
340 alginate. Here, commercially available brown-algae derived alginate was added to Hb101 at a  
341 concentration of 250ug/mL. Experiments were performed in duplicate. The mean +/- SEM is  
342 indicated.

343

344 **Figure 2. The non-mucoid *algT* revertant is significantly more resistant to hydrogen**  
345 **peroxide than the clinical mucoid isolate, FRD1.**

346 (A) Biolog growth curve data for strains grown for 24 hours in the presence of 11.25mM HOCl  
347 (Supplemental Fig 1C) plotted as percent area under the curve (AUC), relative to the no-  
348 treatment condition (B) Biolog data for strains grown in the presence of 25mM H<sub>2</sub>O<sub>2</sub>  
349 (Supplemental Fig 1B) as percent area under the curve (AUC). (C) 1 hour treatment of *P.a.*  
350 strains with 50mM H<sub>2</sub>O<sub>2</sub> plotted as log-fold killing. Experiments were performed in triplicate on  
351 three independent occasions. The mean +/- SEM is indicated. Statistical significance was  
352 measured using an unpaired two-tailed Student's *t*-test. \*p<0.05, \*\*p<0.01, \*\*\*p<0.001

353

354 **Figure 3. Multiple clinical mucoid isolates exhibit sensitivity to H<sub>2</sub>O<sub>2</sub> similar to FRD1.**

355 Biolog growth curve data for strains grown for 24 hours in the presence of 25mM H<sub>2</sub>O<sub>2</sub> plotted  
356 as percent area under the curve (AUC), relative to the no-treatment condition. Dotted line  
357 represents H<sub>2</sub>O<sub>2</sub> sensitivity of FRD1. Strains marked as “ns” were as susceptible as FRD1  
358 to H<sub>2</sub>O<sub>2</sub> (“not significant” statistically compared to FRD1). Experiments were performed in  
359 triplicate on three independent occasions. The mean +/- SEM is indicated. Statistical significance  
360 was measured using an unpaired two-tailed Student's *t*-test. \*\*\*p<0.001

361

362 **Figure 4. Supernatants derived from the *algT* revertant are sufficient to protect mucoid**

363 ***P.a.* from H<sub>2</sub>O<sub>2</sub>-killing via KatA.**

364 (A) Cell-free supernatants derived from the mucoid, *algT*, or *algD* strain were used to resuspend  
365 the mucoid isolate, FRD1, prior to 24-hour growth in the presence of 25mM H<sub>2</sub>O<sub>2</sub> by Biolog.  
366 Supernatants were collected and filter-sterilized from strains after 14-16 hours growth (stationary



367 phase). Supernatants were heat-inactivated (H.I.) at 80 degrees C for 30 minutes. Growth curve  
368 data are plotted as percent area under the curve (AUC), relative to the no-treatment condition.(B)  
369 Supernatants derived from *algT*  $\Delta$ *katA* and *algT*  $\Delta$ *katB* mutants were used to resuspend FRD1  
370 prior to 24-hour growth in presence of H<sub>2</sub>O<sub>2</sub> by Biolog. (C) Supernatants derived from *algT*  
371  $\Delta$ *katA* and *algT*  $\Delta$ *katA* *pkatA* strains were used to resuspend FRD1 prior to 24-hour growth in  
372 presence of H<sub>2</sub>O<sub>2</sub> by Biolog. The mean +/- SEM is indicated. Statistical significance was  
373 measured using an unpaired two-tailed Student's *t*-test.. \**p*<0.05, \*\**p*<0.01, \*\*\**p*<0.001

374

375 **Figure 5. *katA* transcription is negatively regulated by *algT*, via *algR*.**

376 (A) Model for indirect regulation of *katA* transcription by *algT* through one of three downstream  
377 transcription factors, *algB*, *algR*, and *amrZ* (B) Biolog of *P.a.* strains in the presence of 25mM  
378 H<sub>2</sub>O<sub>2</sub>. Data are plotted as percent area under the curve (AUC), relative to the no-treatment  
379 condition. (C) *katA* and *algD* mRNA levels quantitated by RT-PCR, normalized to the mucoid  
380 strain, FRD1. *rpoD* was used as the housekeeping gene in these experiments. (D) Quantitation of  
381 catalase protein activity within cell-free supernatants using BioVision Catalase Activity  
382 Colorimetric Assay Kit. Experiments were performed in triplicate on three independent  
383 occasions. Statistical significance was measured using a two-tailed Student's *t*-test. \**p*<0.05,  
384 \*\**p*<0.01, \*\*\**p*<0.001

385

386 **Figure 6. Deletion of *lys* abrogates protection of mucoid *P.a.* by *algT* supernatants.**

387 (A) *lys* (PA0629) endolysin gene cluster/putative operon (PA0628- PA0632), which mediates  
388 explosive cell lysis and eDNA release in *P.a.* (B) eDNA was visualized by subjecting cell-free  
389 supernatants from *P.a.* strains to 1% agarose gel (with ethidium bromide) electrophoresis. eDNA

390 was observed as high molecular weight (>3000bp) band. (C) eDNA band intensity  
391 (densitometry) was quantitated via ImageJ (D) Supernatants from *algT* and *algT*  $\Delta$ *lys* mutants  
392 were used to resuspend FRD1 prior to 24-hour growth in presence of H<sub>2</sub>O<sub>2</sub> (E) *lys* mRNA levels  
393 quantitated by RT-PCR, relative to the mucoid strain, FRD1 (F) Quantitation of catalase protein  
394 activity within cell-free supernatants using BioVision Catalase Activity Colorimetric Assay Kit.  
395 Experiments were performed in triplicate on three independent occasions. Statistical significance  
396 was measured using a two-tailed Student's *t*-test. \**p*<0.05, \*\**p*<0.01, \*\*\**p*<0.001

397

398 **Figure 7. Mucoid and non-mucoid *P.a.* variants in co-culture exhibit enhanced resistance to**  
399 **both H<sub>2</sub>O<sub>2</sub> and LL-37.** (A) Mono- and co-cultures of mucoid strain, FRD1, and *algT* revertant  
400 exposed to 25mM H<sub>2</sub>O<sub>2</sub> for 1 hour. Mucoid strain used was a spontaneous streptomycin resistant  
401 isolate and the non-mucoid *algT* revertant was a spontaneous rifampicin resistant isolate.  
402 Surviving bacteria were enumerated by plating on respective (antibiotic-containing) medium to  
403 differentiate between mucoid and *algT* strains. Percent survival was calculated relative to the no-  
404 treatment condition for each strain. (B) Mono- and co-cultures of FRD1, and *algD* mutant  
405 exposed to 50ug/mL LL-37 for 1 hour. Mucoid strain used was a spontaneous streptomycin  
406 resistant isolate and the non-mucoid *algD* mutant was a spontaneous rifampicin resistant isolate.  
407 Data are represented as log-fold killing compared to no-treatment for each strain/condition.  
408 Experiments were performed in duplicate on three independent occasions. Statistical significance  
409 was measured using a two-tailed Student's *t*-test. \**p*<0.05, \*\**p*<0.01

410

411 **Figure 8. Model for mucoid/non-mucoid revertant co-existence in the CF lung.** Mucoid *P.a.*  
412 provides multi-variant community protection from LL-37 via alginate production. Non-mucoid  
413 members of the community provide protection from H<sub>2</sub>O<sub>2</sub> via catalase production.

414

415 **Supplemental Figure 1. The non-mucoid *algT* revertant is more resistant to growth in the**  
416 **presence of H<sub>2</sub>O<sub>2</sub> compared to the isogenic mucoid isolate, FRD1.**

417 (A) 24 hour Biolog growth curves of mucoid strain, FRD1 (*mucA*), isogenic *algT* and *algD*  
418 mutants grown in the presence of medium alone (B) 24 hour Biolog growth curves of *P.a.*  
419 strains-of-interest in the presence of 25mM H<sub>2</sub>O<sub>2</sub> (C) Biolog growth curves of *P.a.* strains in the  
420 presence of 11.25mM HOCl. Experiments were performed in triplicate on three independent  
421 occasions. The mean growth reading per hour across three independent experiments is indicated.

422

423

424

425

426

427

428

## 429 **References**

- 430 1. Spoonhower, K. A. & Davis, P. B. Epidemiology of Cystic Fibrosis. *Clin. Chest Med.* **37**,  
431 1–8 (2016).
- 432 2. Cystic Fibrosis Foundation. Patient Registry. Annual Data Report 2012. 28 (2012).
- 433 3. Langton Hewer SC. Smyth, A. Antibiotic strategies for eradicating *Pseudomonas*

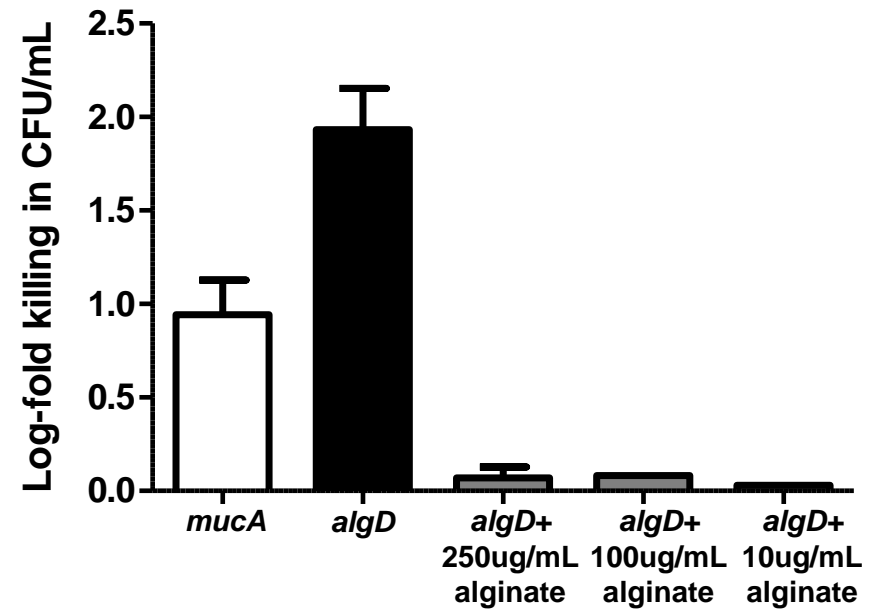
- 434 aeruginosa in people with cystic fibrosis. [Review] [60 refs][Update of Cochrane Database  
435 Syst Rev. 2006;(1):CD004197; PMID: 16437476]. *Cochrane Database Syst. Rev.* (2009).  
436 doi:10.1002/14651858.CD004197.pub3.Copyright
- 437 4. Moreau-Marquis, S., Stanton, B. A. & O'Toole, G. A. Pseudomonas aeruginosa biofilm  
438 formation in the cystic fibrosis airway. *Pulm. Pharmacol. Ther.* **21**, 595–9 (2008).
- 439 5. Bendiak, G. N., Ratjen, F. & Ph, D. The Approach to Pseudomonas aeruginosa in Cystic  
440 Fibrosis. *Crit. Care* **1**, 587–595 (2009).
- 441 6. Brennan, S. Innate immune activation and cystic fibrosis. *Paediatr. Respir. Rev.* **9**, 271–  
442 280 (2008).
- 443 7. Galli, F. *et al.* Oxidative stress and antioxidant therapy in cystic fibrosis. *Biochim.*  
444 *Biophys. Acta* **1822**, 690–713 (2012).
- 445 8. Ciofu, O., Tolker-Nielsen, T., Jensen, P. ??strup, Wang, H. & H??iby, N. Antimicrobial  
446 resistance, respiratory tract infections and role of biofilms in lung infections in cystic  
447 fibrosis patients. *Adv. Drug Deliv. Rev.* (2014). doi:10.1016/j.addr.2014.11.017
- 448 9. Boucher, J. C., Yu, H., Mudd, M. H. & Deretic, V. Mucoïd Pseudomonas aeruginosa in  
449 cystic fibrosis : characterization of muc mutations in clinical isolates and analysis of  
450 clearance in a mouse model of respiratory infection . Mucoïd Pseudomonas aeruginosa in  
451 Cystic Fibrosis : Characterization of muc Muta. **65**, 3838–3846 (1997).
- 452 10. Govan, J. R. & Deretic, V. Microbial pathogenesis in cystic fibrosis: mucoïd  
453 Pseudomonas aeruginosa and Burkholderia cepacia. *Microbiol. Rev.* **60**, 539–574 (1996).
- 454 11. Hengzhuang, W., Wu, H., Ciofu, O., Song, Z. & Høiby, N.  
455 Pharmacokinetics/pharmacodynamics of colistin and imipenem on mucoïd and nonmucoïd  
456 Pseudomonas aeruginosa biofilms. *Antimicrob. Agents Chemother.* **55**, 4469–4474 (2011).

- 457 12. Li, Z. *et al.* Infection and Lung Disease Progression in Children With Cystic Fibrosis. **293**,  
458 581–588 (2005).
- 459 13. Brown, S. M., Howell, M. L., Vasil, M. L., Anderson, A. J. & Hassett, D. J. Cloning and  
460 characterization of the katB gene of Pseudomonas aeruginosa encoding a hydrogen  
461 peroxide-inducible catalase: purification of KatB, cellular localization, and demonstration  
462 that it is essential for optimal resistance to hydrogen peroxide. *J. Bacteriol.* **177**, 6536–44  
463 (1995).
- 464 14. Ciofu, O. & Bjarnsholt, T. Pseudomonas aeruginosa biofilms in Cystic Fibrosis. *Future*  
465 *Microbiol.* **5**, 1663–1674 (2010).
- 466 15. Ciofu, O. *et al.* Investigation of the algT operon sequence in mucoid and non-mucoid  
467 Pseudomonas aeruginosa isolates from 115 Scandinavian patients with cystic fibrosis and  
468 in 88 in vitro non-mucoid revertants. *Microbiology* **154**, 103–113 (2008).
- 469 16. Martin, D. W. *et al.* Mechanism of conversion to mucoidy in Pseudomonas aeruginosa  
470 infecting cystic fibrosis patients. *Proc. Natl. Acad. Sci. U. S. A.* **90**, 8377–81 (1993).
- 471 17. Damkiaer, S., Yang, L., Molin, S. & Jelsbak, L. Evolutionary remodeling of global  
472 regulatory networks during long-term bacterial adaptation to human hosts. *Proc Natl Acad*  
473 *Sci U S A* **110**, 7766–7771 (2013).
- 474 18. Xu, B., Soukup, R. J., Jones, C. J., Fishel, R. & Wozniak, D. J. Pseudomonas aeruginosa  
475 AmrZ binds to four sites in the algD promoter, inducing DNA-AmrZ complex formation  
476 and transcriptional activation. *J. Bacteriol.* **198**, 2673–2681 (2016).
- 477 19. Heckman, K. L. & Pease, L. R. Gene splicing and mutagenesis by PCR-driven overlap  
478 extension. *Nat Protoc* **2**, 924–932 (2007).
- 479 20. Jones, C. J., Ryder, C. R., Mann, E. E. & Wozniak, D. J. AmrZ modulates pseudomonas

- 480 aeruginosa biofilm architecture by directly repressing transcription of the psl operon. *J.*  
481 *Bacteriol.* **195**, 1637–1644 (2013).
- 482 21. Limoli, D. H. *et al.* Cationic Antimicrobial Peptides Promote Microbial Mutagenesis and  
483 Pathoadaptation in Chronic Infections. *PLoS Pathog.* **10**, (2014).
- 484 22. Pedersen, S. S., Kharazmi, A., Espersen, F. & Hoiby, N. Pseudomonas aeruginosa alginate  
485 in cystic fibrosis sputum and the inflammatory response. *Infect. Immun.* **58**, 3363–3368  
486 (1990).
- 487 23. Leid, J. G. *et al.* The exopolysaccharide alginate protects Pseudomonas aeruginosa biofilm  
488 bacteria from IFN-gamma-mediated macrophage killing. *J. Immunol.* **175**, 7512–7518  
489 (2005).
- 490 24. Britigan, B. E. *et al.* Antioxidant Enzyme Expression in Clinical Isolates of Pseudomonas  
491 aeruginosa : Identification of an Atypical Form of Manganese Superoxide Dismutase. **69**,  
492 7396–7401 (2001).
- 493 25. Heo, Y.-J. *et al.* The major catalase gene (katA) of Pseudomonas aeruginosa PA14 is  
494 under both positive and negative control of the global transactivator OxyR in response to  
495 hydrogen peroxide. *J. Bacteriol.* **192**, 381–90 (2010).
- 496 26. Turnbull, L. *et al.* Explosive cell lysis as a mechanism for the biogenesis of bacterial  
497 membrane vesicles and biofilms. *Nat. Commun.* **7**, 11220 (2016).
- 498

Figure 1

A.



B.

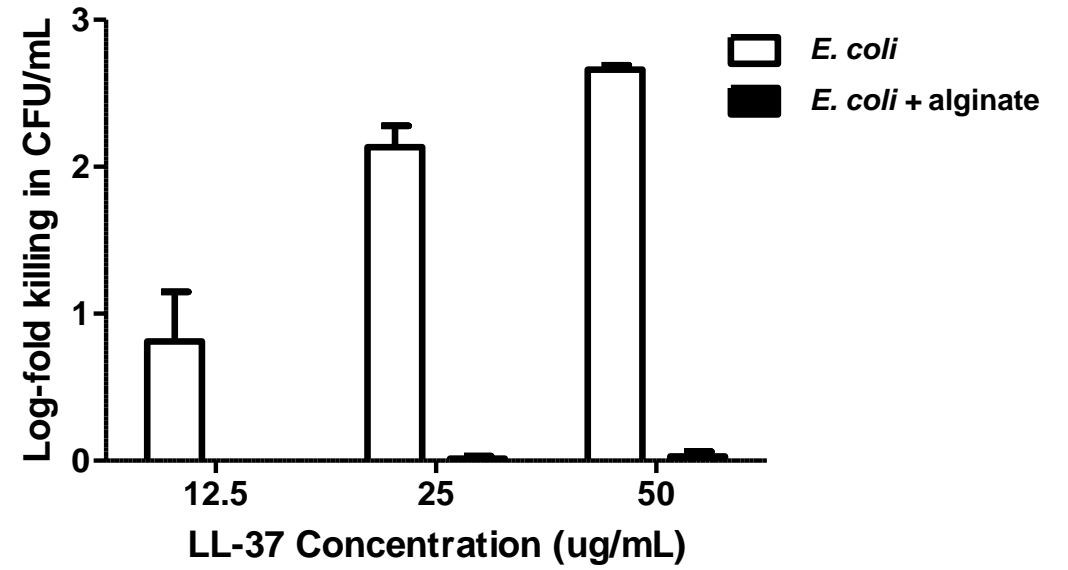


Figure 2

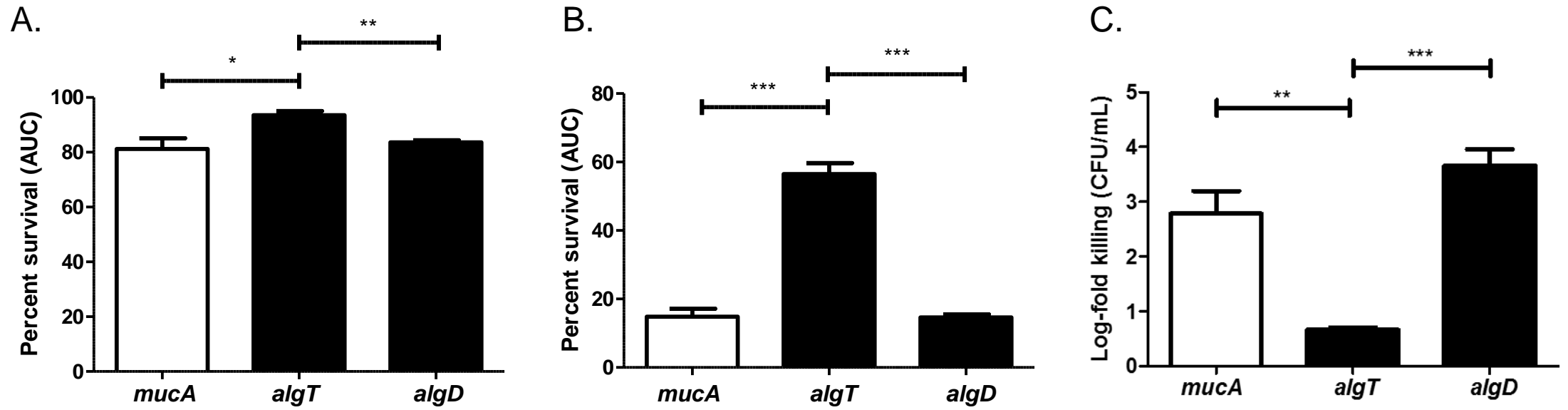




Figure 3

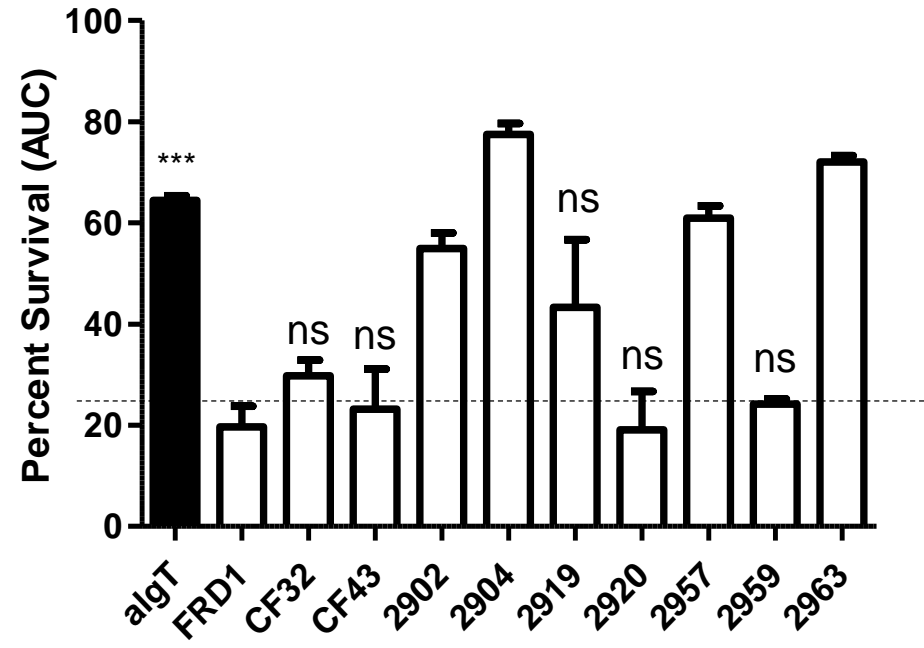


Figure 4

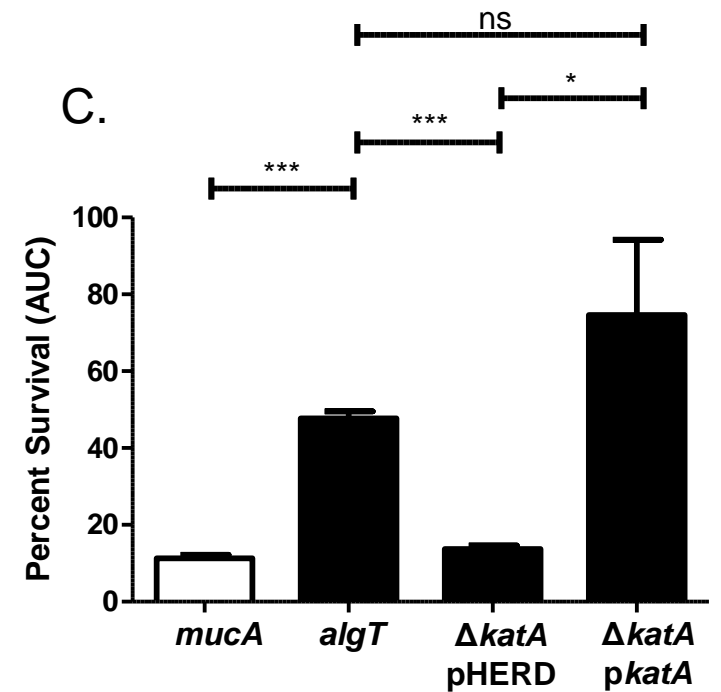
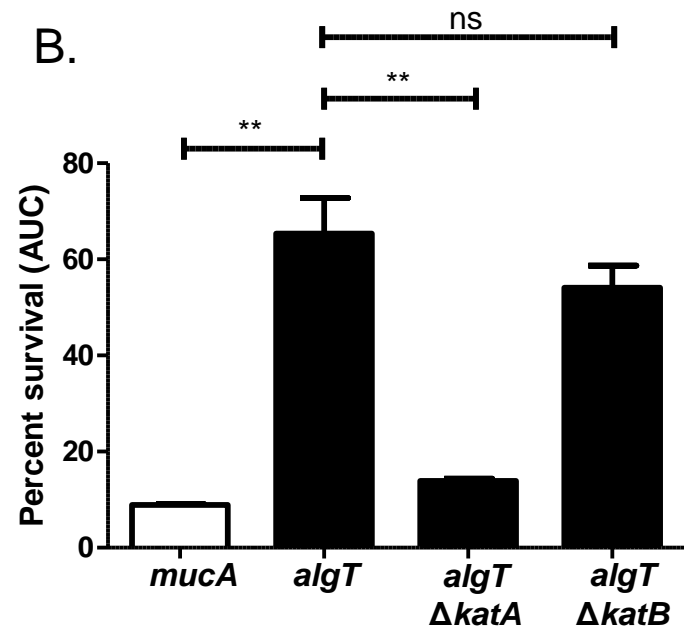
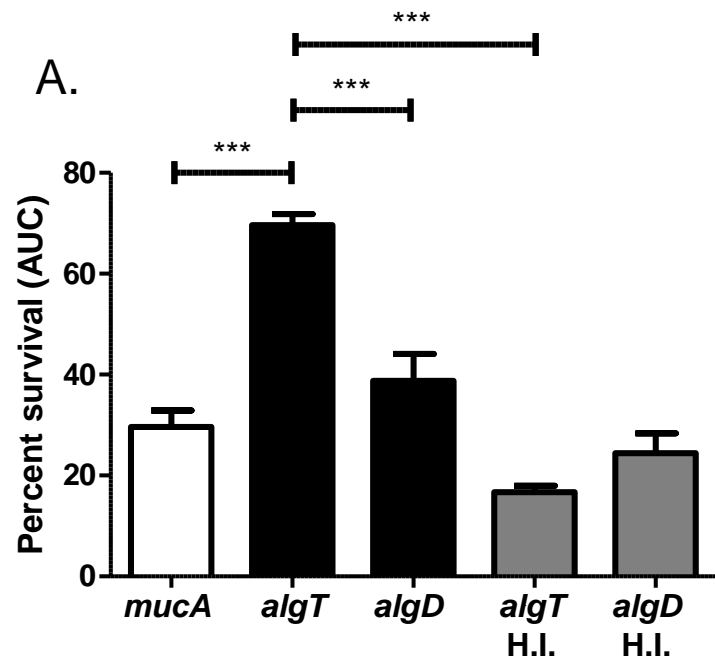
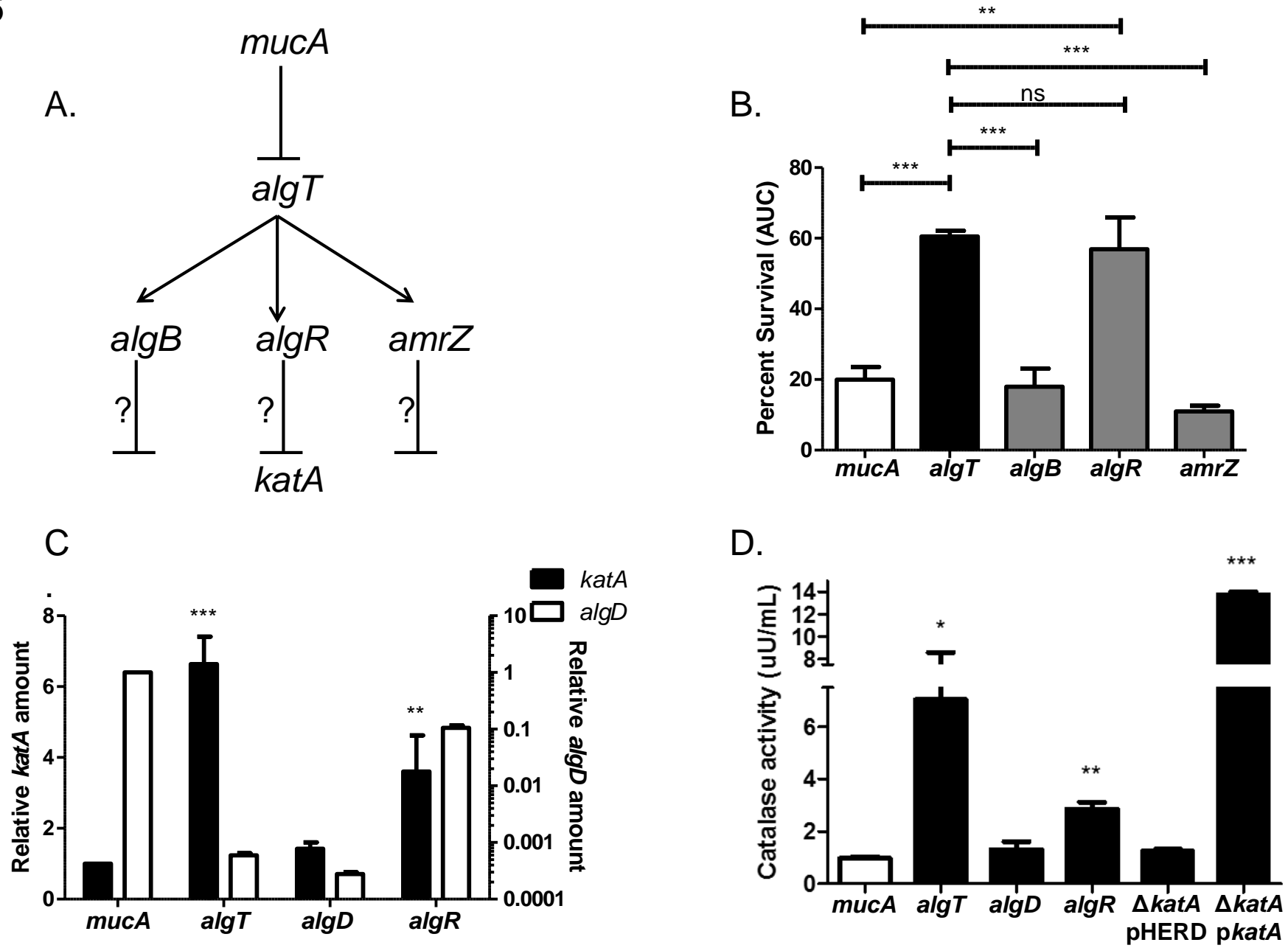


Figure 5



**Figure 6**

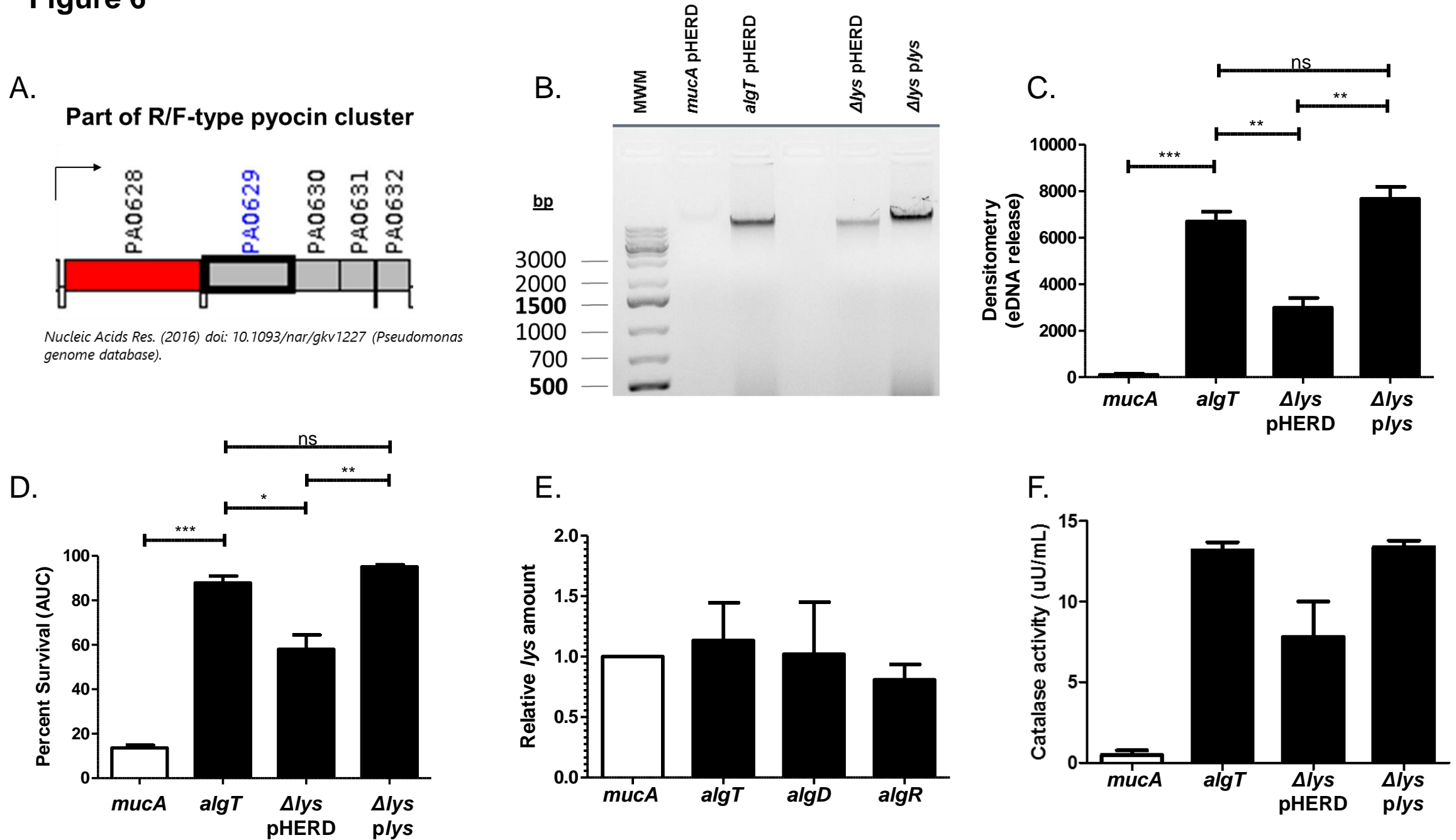
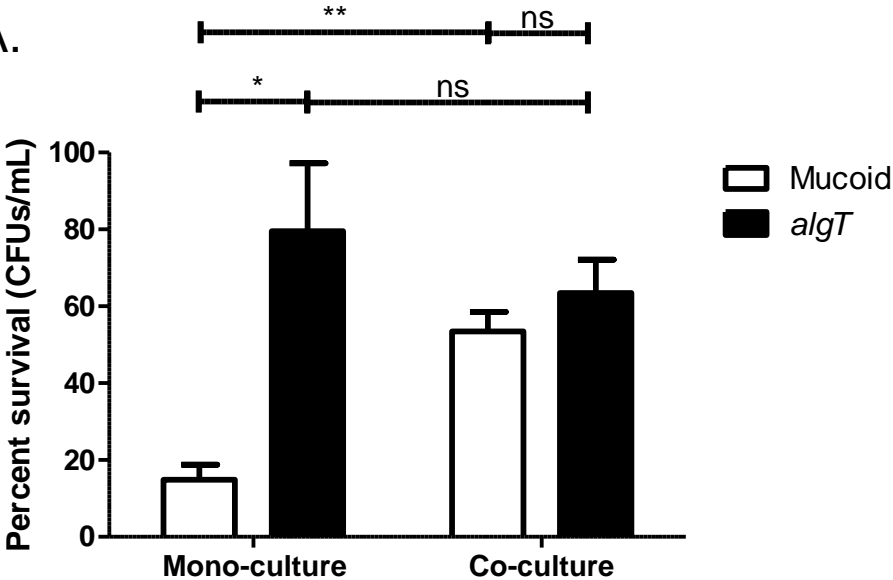


Figure 7

A.



B.

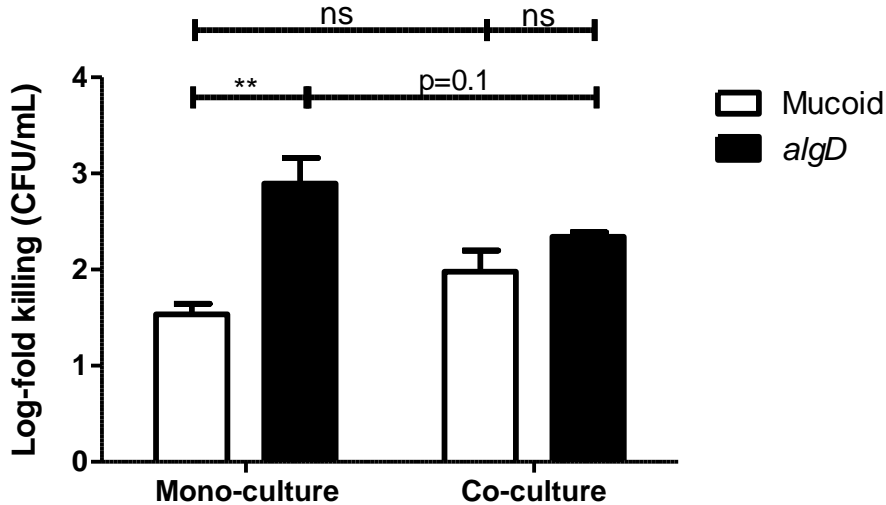
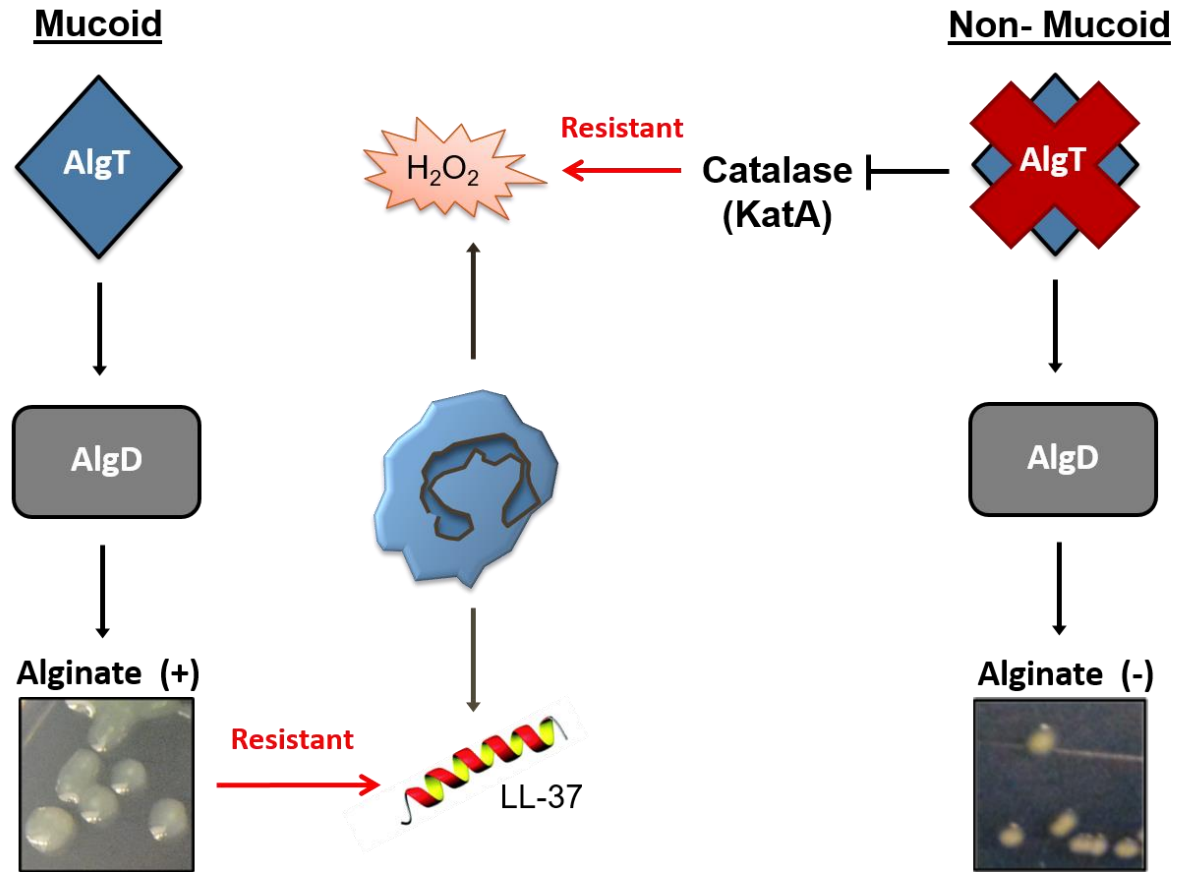


Figure 8



# Supplemental Figure 1

